

This version of the article has been accepted for publication, after peer review and is subject to Springer Nature's AM terms of use, but is not the Version of Record and does not reflect post-acceptance improvements, or any corrections. The Version of Record is available online at: <https://doi.org/10.1007/s00259-018-4183-0>.

Title: Myocardial MIBG scintigraphy in genetic Parkinson's disease as a model for Lewy body disorders

Authors: Iñigo Gabilondo^{1*}, Verónica Llorens^{1,2}, Trinidad Rodriguez², Manuel Fernández^{1,3,4}, Tomas Pérez Concha³, Marian Acera¹, Beatriz Tijero¹, Ane Murueta-Goyena¹, Rocío del Pino¹, Jesús Cortés⁵, Juan Carlos Gómez-Esteban^{1,3,4}

¹Neurodegenerative Diseases Group, Biocruces Health Research Institute, Barakaldo, Bizkaia, Spain; ²Nuclear Medicine Department, Cruces University Hospital, Barakaldo, Bizkaia, Spain; ³Neurology Department, Cruces University Hospital, Barakaldo, Bizkaia, Spain; ⁴Department of Neurosciences, University of the Basque Country, Leioa, Spain; ⁵Computational Neuroimaging Group, Biocruces Health Research Institute, Barakaldo, Bizkaia, Spain

***Corresponding author:**

Iñigo Gabilondo, Neurodegenerative Diseases Group, Biocruces Health Research Institute, Plaza de Cruces 12, Barakaldo (Bizkaia), CP 48903, Spain.

Corresponding author's phone and fax: +34 946006000 ext. 7970

Corresponding author's e-mail: igabilon@gmail.com

Running head: Myocardial MIBG scintigraphy in genetic Parkinson's disease

Word count: Abstract: 265; Text: 3358; **References:** 31; **Tables:** 2; **Figures:** 2.

Keywords: Parkinson's disease; MIBG cardiac scintigraphy; dysautonomia; genetic; alpha-synuclein.

Contributors: IG, VL and JCG designed the study, and IG, VL, TR, JCG, AM and BT collected the data. IG, VL and JCG supervised the study. IG, JC and JCG did the statistical analysis, while IG and VL created figures and tables. IG, VL and JCG interpreted the results of the analysis with subsequent substantial contributions from all the co-authors. IG, VL and JCG drafted the manuscript, to which all the authors contributed with revisions and approved the final version.

Abstract

Purpose: to identify myocardial sympathetic denervation patterns suggestive of Lewy body (LB) pathology in genetic and idiopathic parkinsonisms by ^{123}I -metaiodobenzylguanidine (MIBG) scintigraphy.

Methods: we retrospectively analysed myocardial MIBG images acquired with a dual-head gamma camera and low-energy high-resolution collimator (LEHR) in 34 genetic Parkinson's disease (PD; 4 PARK1, 8 PARK2 and 22 PARK8), 85 with idiopathic PD (iPD), 6 with idiopathic REM sleep behaviour disorder (iRBD), 17 with dementia with LB (DLB), 40 with multiple system atrophy (MSA), 12 with progressive supranuclear palsy (PSP) and in 45 controls. We calculated heart-to-mediastinum MIBG uptake ratios (HMR) at 15 min and 4 hours (HMR4H) for LEHR and for standardized medium energy collimators, obtaining HMR classification accuracies and optimal cut-off values with supervised classification and ROC analyses.

Results: while patients with LB disorders had markedly lower $\text{HMR4H}_{\text{LEHR}}$ than controls (controls: 1.86 ± 0.26 , iPD: 1.37 ± 0.29 , iRBD: 1.23 ± 0.09 , PARK1: 1.20 ± 0.09 ; DLB: 1.17 ± 0.11 ; $p < 0.05$), for the remaining categories differences were smaller (PARK8: 1.51 ± 0.32 ; $p < 0.05$) or non-significant (MSA: 1.82 ± 0.37 , PSP: 1.59 ± 0.23 , PARK2: 1.51 ± 0.30 ; $p > 0.05$). The diagnostic accuracy of $\text{HMR4H}_{\text{LEHR}}$ was highest for LB disorders (PARK1, iPD, DLB, iRBD) (89 to 97 %) and lowest for PARK2, PARK8, PSP and MSA (65 to 76 %), with an optimal $\text{HMR4H}_{\text{LEHR}}$ cut-off value of 1.72 for discriminating patients with most LB disorders including iPD and 1.40 for aggressive LB spectrum phenotypes (DLB, PARK1 and iRBD).

Conclusions: Our study including patients with a wide spectrum of genetic and idiopathic parkinsonisms with different degrees of LB pathology further supports myocardial MIBG scintigraphy as an accurate tool for discriminating patients with LB spectrum disorders.

Introduction

Metaiodobenzylguanidine (MIBG) is a physiological analogue of noradrenaline, which is actively transported and stored into granules in presynaptic sympathetic nerve endings. Myocardial ¹²³I-MIBG uptake correlates with the integrity of postganglionic sympathetic cardiac nerves being able to quantify non-invasively the extent of myocardial denervation in synucleinopathies and in atypical parkinsonisms, helping with the differential diagnosis [1]. Several myocardial ¹²³I-MIBG scintigraphy studies have consistently demonstrated decreased myocardial noradrenergic innervation in idiopathic Parkinson's disease (iPD)[2], pure autonomic failure, idiopathic REM sleep behaviour disorder (iRBD)[3] and dementia with Lewy bodies (DLB). In contrast, in patients with atypical parkinsonism, such as multiple system atrophy (MSA) or progressive supranuclear palsy (PSP), myocardial scintigraphy results are normal in a high proportion of patients [4]. Interestingly, the clinical phenotypes with highest risk to develop a diffuse and severe Lewy body (LB) pathology in the CNS are those with highest degrees of myocardial denervation in MIBG imaging studies [5-8]. Genetic variants of PD include relatively homogenous groups of patients from the clinical and neuropathological point of view, including patients with aggressive LB pathology like alpha-synuclein gene mutation carriers (SNCA) (PARK1)[9], patients with variable degree of LB disease such as Leucine-Rich Repeat Kinase 2 gene mutation carriers (LRRK2) (PARK8) and patients virtually free of LB pathology like Parkin gene mutation carriers (PARK2). The use of myocardial MIBG scintigraphy in such genetic groups may provide additional evidences to further validate the diagnostic performance of MIBG scintigraphy as an early biomarker of LB spectrum disorders [10-13]. The aim of the present study is to evaluate the degree of myocardial sympathetic denervation as measured by MIBG scintigraphy in a wide spectrum of genetic and idiopathic parkinsonisms and related disorders, with a special interest in comparing

MIBG denervation trends in phenotypes with severe LB pathology (PARK1 carriers, DLB and iRBD) and those with less or absent LBs (PARK2 carriers, MSA, PSP and controls). We also aimed to identify the optimal cut-off values for myocardial MIBG metrics and their respective accuracies to discriminate healthy individuals from parkinsonisms.

Materials and Methods

Study design and selection of participants

We analysed retrospectively all patients with suspected synucleinopathy or atypical parkinsonism that underwent myocardial MIBG scintigraphy for clinical purposes in the Movement Disorder Unit and Nuclear Medicine Department of Cruces University Hospital between years 2007 and 2017. We identified 34 patients with genetic PD [all symptomatic mutation carriers, including E46K-SNCA (PARK1) (n=4), PARK2 (n=8) and PARK8 (n=22)], 87 iPD, 6 iRBD (probable or polysomnography confirmed), 17DLB, 40 probable MSA and 12 probable PSP. We did not include in this study patients with levodopa resistant iPD because of their pathophysiological peculiarities as compared to classic levodopa responsive iPD [14]. We also selected 45 healthy controls (HC) that underwent MIBG scintigraphy for clinical purposes as a routine screening for suspicion of neurovascular dysautonomia. We reviewed all electronic clinical records to gather basic demographical data and disease-related information. We also identified a set of factors different from LB pathology influencing structural or functional integrity of myocardial innervation, excluding all subjects with known heart failure (or other structural heart disease) and microvascular diabetic complications. In order to further rule out heart failure or segmental myocardial function or perfusion defects, in addition to MIBG scintigraphy, all subjects underwent ECG-gated myocardial Technetium (99mTc) 6-methoxy isobutyl isonitrile (6-MIBI) single-photon emission computerized tomography (SPECT) under rest conditions. Two expert nuclear medicine specialists (VL and TR) analysed ECG-gated 99mTc-6-MIBI SPECT images identifying and quantifying abnormalities in global and regional myocardial perfusion, left ventricle ejection fraction, total diastolic and systolic volumes and identified ventricular wall movement abnormalities. For simplicity, in this study we excluded all subjects for who analysis of resting 99mTc-6-MIBI images revealed impaired left ventricle function

(ejection fraction below 50%), severe regional myocardial hypoperfusion and/or ventricular wall movement abnormalities consistent in distribution with any known coronary territory, if it was not contradicted by subsequent cardiological evaluations, assuring myocardial structural and functional integrity. Lastly, unless strictly necessary for medical reasons, all subjects were asked to discontinue 7 days prior to MIBG imaging any sympathicomimetics, antihypertensive drugs, tricyclic antidepressants and antipsychotics known to affect MIBG uptake [15]. All participants signed a specific written informed consent for myocardial imaging and for the codified recording of their clinical and imaging data in the registry of our Movement Disorder Unit. The protocol of this study was approved by the local ethics committee.

Myocardial imaging acquisition and analysis

Myocardial ^{123}I -MIBG scintigraphy and ECG-gated $^{99\text{m}}\text{Tc}$ -6-MIBI SPECT images were acquired with a dual head gamma camera system (Infinia, GE Healthcare, Milwaukee, USA) equipped with a low-energy high-resolution (LEHR) parallel-hole collimator. The acquisition and analysis of myocardial MIBG images were performed according to standard guidelines [16]. A detailed description of our protocols, both for MIBG scintigraphy and ECG-gated $^{99\text{m}}\text{Tc}$ -6-MIBI SPECT can be found in Supplementary materials together with illustrative MIBG examples. Regarding MIBG image quantification, both for early and delayed anterior MIBG images, two nuclear medicine specialists (VL and TR) manually drawn regions of interest (ROIs) of heart, lung and upper mediastinum (avoiding thyroid gland). The mean count density for each ROI was obtained and the heart / mediastinum ratios (HMR) were calculated for MIBG uptake in early (15 min) and delayed (4 hours) phases (from now on, respectively referred in this manuscript as HMR15M and HMR4H). In order to obtain a measure of the balance between intraneuronal and extraneuronal binding and clearance of myocardial MIBG (sympathetic neuron activity and integrity in the heart) we calculated myocardial MIBG washout percentage with the following formula: $[(\text{HMR}_{15\text{M}}^{\text{LEHR}} - \text{HMR}_{4\text{H}}^{\text{LEHR}}) / \text{HMR}_{15\text{M}}^{\text{LEHR}}] * 100$. Instead of using the subtraction of background (mediastinum) counts from heart counts as previously reported[8] in the present work we used the ratios of heart to mediastinum MIBG uptake to calculate early to late myocardial MIBG washout. Lastly, since the characteristics of the collimator are major factors influencing variations among institutions and studies for the calculation of HMR [for example, medium energy (ME) collimators show higher HMR

values than those estimated on low energy (LE) collimators[17]] and taking into account the widespread application and the recommendations of use of ME collimators for estimation of HMR in myocardial ¹²³I-MIBG imaging [16], for generalization purposes, in the present study the HMR values were estimated both as the raw LEHR HMR values obtained with our LEHR collimator (HMR15M_{LEHR} and HMR4H_{LEHR}) and as the standardized HMR values for ME collimators (HMR15M_{STD} and HMR4H_{STD}) calculated with the formula and conversion factor for LEHR (0.553) provided in the cross-calibration phantom study by Verschure et al [18].

Data analysis, classification accuracy and optimal MIBG cut-off values

We first calculated proportions, means and standard deviations and assessed differences between diagnostic categories with Kruskal-Wallis ANOVA test for continuous variables (age, disease duration and MIBG metrics) and pair-wise Fisher's exact test for categorical variables (gender and presence of diabetes) using SPSS Statistics for Windows Version 20.0 (IBM Corp., Armonk, NY, USA). We ranked diagnostic categories according to their respective median HMR4H values following Jonckheere-Terpstra non-parametric rank test (see figure 1) and we grouped them in clusters to test the diagnostic performance of HMR in nine different classification strategies (S1 to S9) (see table 2). We calculated the optimal cut-off values for HMR4H (HMR4H_{LEHR} and HMR4H_{STD}) and HMR15M (HMR15M_{LEHR} and HMR15M_{STD}) in each classification scheme (S1 to S9) using two approaches: 1) Maximization of discrimination accuracy with the supervised classification algorithm "classification and regression tree" (CART); 2) Maximization of discrimination sensitivity and specificity with non-parametric receiver operating characteristic (ROC) analyses. Since each approach aims to maximize different classification parameters, discrepancies in cut-off values were expected [19]. We implemented CART in the Waikato Environment for Knowledge Analysis (WEKA)[20] obtaining for each classification strategy baseline accuracy (proportion of patients with respect to the total number of subjects within each strategy) (Bs-Accuracy), CART training accuracy (Total Tr-Accuracy) and CART K-fold (K=10) cross-validation accuracy (Cv-Accuracy). ROC analyses were implemented under SPSS, obtaining for each classification scheme ROC curves, areas under the curve (AUC) and the optimal cut-off values with respective sensitivities and specificities by maximizing the value of Youden's index[21]. See Supplementary materials for further descriptions on methodology for data analysis.

Results

As the first main result of our study, we observed a clear-cut spectrum of progressive myocardial MIBG uptake deficit, both for HMR15M and HMR4H, that was related to the severity of LB pathology attributed to each diagnostic category, with the highest average HMR values found in HC, MSA and PSP and the lowest ones in iPD, iRBD and DLB (see Table 01 and Figure 01). Furthermore, we did not observe statistically significant differences in HMR values between genetic PD variants known to have mild or absent LB pathology (PARK2) and MSA or HC. Similarly, we did not find significant differences ($p > 0.05$) in HMR values between genetic carriers with severe LB disease (PARK1) and iRBD or DLB.

As the second main finding of our study, CART and ROC analyses demonstrated that HMR4H (and not HMR15M) provided excellent performance to differentiate controls from patients with moderate to severe LB pathology (Table 2 and Figure 2). Moreover, the classification algorithms found that the most optimal $HMR4H_{LEHR}$ cut-off value to discriminate most LB spectrum disorders including iPD patients was 1.72 ($HMR4H_{STD}$ of 2.15) and that the best $HMR4H_{LEHR}$ cut-off value to additionally differentiate the most aggressive LB spectrum phenotypes (iRBD, PARK1 and DLB) was 1.40 ($HMR4H_{STD}$ of 1.64). Conversely, lowest HMR4H classification accuracies (and lowest improvements from baseline accuracies) were obtained for strategies including exclusively parkinsonisms with mild or absent LB pathology (PARK8, PARK2, PSP and MSA). The latter was especially true when HMR4H values of MSA patients were compared with controls. In fact, in CART analyses for most HMR4H classification strategies including MSA the optimal cut-off value was undetermined, supporting the existence of marked differences between MSA and the other groups.

Table 1 summarizes demographical and clinical characteristics of study population. All groups were comparable in age and gender, with no statistically significant differences except for age in DLB patients, that were older than PARK1 carriers and healthy controls. The prevalence of diabetes mellitus was comparable between groups (averaged from 12.5% to 16.7%) except for PSP group for who it was higher but not statistically significant. The disease duration averaged from 3.55 to 5.62 years, with no statistically significant group differences except for PARK2 and PARK8, that had significantly longer disease durations. HMR washout was in line with the pattern observed for

separated HMR values, with the lowest HMR washout percentages identified in HC and MSA and the highest ones in iPD, PARK1 and DLB. We did not find statistically significant differences in myocardial MIBG metrics between diabetic and non-diabetic participants within each group (data not shown). We also evaluated the correlation between MIBG measures, age and disease duration in patients, finding that age (and not disease duration) was significantly ($p < 0.05$) correlated with HMR15M and HMR4H in all study groups.

Regarding the classification performance of the identified optimal HMR4H_{LEHR} cut-off values, according to the HMR4H_{LEHR} cut-off value of 1.40 (HMR4H_{STD} 1.64), in our study population myocardial MIBG would be classified as abnormal in 2 HC (4.4%), 5 MSA (12.5%), 2 PSP (16.7%), 2 PARK2 (25.0%), 11 PARK8 (50.0%), 47 iPD (54.0%), 6 iRBD (100%), 17 DLB (93.3%) and 4 PARK1 (100%). For a HMR4H_{LEHR} cut-off value of 1.72 (HMR4H_{STD} 2.15), myocardial MIBG would be classified as abnormal in 6 HC (13.3%), in 15 MSA (37.5%), in 8 PSP (66.7%), in 5 PARK2 (62.5%), in 16 PARK8 (72.7%), in 74 iPD (85.1%), in 6 iRBD (100%), in 17 DLB (100%) and in 4 PARK1 (100%).

Lastly, for the analyses of the diagnostic accuracy with HMR15M values, in ROC analyses we found a similar pattern to HMR4H in which HMR15M had highest accuracies when including exclusively patients with highest LB pathology (PARK1, DLB, iRBD and iPD) (AUC above 0.91) and lowest accuracies when exclusively participants with mild or absent LB pathology (PARK8, PARK2, PSP and MSA) were included (AUC below 0.66). However, the diagnostic performance of HMR15M in terms of specificity and identification of possible cut-off values in ROC analyses and CART was much worse than for HMR4H (see Supplementary Figure 2 and Supplementary Table for further details).

Discussion

In the present study we analysed myocardial MIBG scintigraphy patterns in a wide variety of idiopathic and genetic parkinsonisms characterized for having different degrees of LB pathology. Our results, supported by the inclusion of genetic PD variants, further validates the usefulness of myocardial MIBG scintigraphy to discriminate LB spectrum disorders (PARK1, DLB, iRBD and iPD) both from healthy controls and from parkinsonisms with milder or absent LB pathology (PARK2,

PSP or MSA). Furthermore, we observed that in our center an HMR4H_{LEHR} cut-off value below 1.40 (HMR4H_{STD} of 1.64) would correctly identify 93.3% to 100% of most aggressive LB diseases (PARK1, DLB and iRBD) and a HMR4H_{LEHR} cut-off value below 1.72 (HMR4H_{STD} of 2.15) would additionally discriminate up to 85.1% of iPD cases.

The analysis of genetic PD variants has enabled us to study homogenous patient groups, including genotypes with high LB burden (PARK1 mutations), genetic variants with varying degrees of LB pathology (PARK8) and cases with mild or absent LB (PARK2). Previous studies performed by our group support that the analysis of neurovascular dysfunction and myocardial sympathetic denervation may be helpful to differentiate PD genotypes with marked LB pathology [10, 12, 22], which is in line with other studies demonstrating myocardial denervation in idiopathic LB spectrum disorders [3, 6, 23, 24]. The present study also demonstrates that myocardial MIBG imaging is helpful to differentiate MSA patients from iPD cases, as previously stated even for early disease stages [4, 25]. Our study also illustrates the presence of exceptions in MIBG uptake patterns. For example, while as expected most iPD patients (54.0 to 85.1 %) had abnormal MIBG and most MSA patients (62.5 to 87.5 %) had normal MIBG, there was a considerable number of patients in both groups not following this pattern. In our study, MIBG measures were not significantly related with disease duration or other influencing factors such as diabetes or heart disease. In iPD patients, one of the potential influencing factors for MIBG misclassification may be related with the well-known clinical and pathogenic variability of iPD [26], which might be linked to the variability of LB pathology in iPD and, hence, to the variability in the degree of myocardial denervation. In line with this idea, we believe that myocardial MIBG might be a good tool to identify iPD cases heavily driven by LB pathology. In the case of MSA patients with abnormal myocardial MIBG imaging, although the reasons for this finding remains unknown, some authors have suggested that it may be due to trans-synaptic degeneration or to a concomitant LB disorder [27]. Other authors have also suggested that MSA patients may develop LBs over the years [28], in fact LBs have been observed in sympathetic ganglia of some MSA patients, potentially favouring lower myocardial MIBG uptake [29].

We found that the use of HMR4H had an outstanding classification accuracy to differentiate LB disorders from HC. Moreover, we found that in our centre a HMR4H_{LEHR} cut-off value of 1.40 (HMR4H_{STD} of 1.64) was optimal for discriminating HC from the most aggressive LB disorders (DLB,

PARK1 and iRBD) and that a $HMR4H_{LEHR}$ cut-off value of 1.72 ($HMR4H_{STD}$ of 2.15) was optimal to identify also most iPD cases. In fact, our findings are comparable to the results obtained in a comprehensive meta-analysis comprising 46 myocardial ^{123}I -MIBG publications using similar imaging equipments (triple- or double-headed gamma camera with LEHR collimators) and including a total of 2680 participants with varied neuro-psychiatric and movement disorders [30]. In the former study, they concluded that the best $HMR4H_{LEHR}$ threshold to discriminate a cluster of LB disorders (PD, DLB and iRBD) from another cluster of CNS neurodegenerative conditions with low or absent LB pathology (Alzheimer's disease, MSA, PSP, vascular dementia and frontotemporal dementia) was 1.77, which is close to the optimal $HMR4H_{LEHR}$ cut-off value of 1.72 that we found to discriminate healthy controls (absent LB pathology) from patients with LB disorders (iPD, iRBD, DLB and PARK1). Regarding the optimal $HMR4H_{LEHR}$ cut-off value of 1.40 that we found to differentiate severe LB disorders (iRBD, DLB and PARK1) from controls, although the meta-analysis did not provide specific $HMR4H_{LEHR}$ thresholds to discriminate most severe LB disease phenotypes, it is worth mentioning that in most individual studies of the meta-analysis including DLB and iRBD their average $HMR4H_{LEHR}$ values were below 1.40.

One of the strongest methodological advantages of our study is related to our approaches to exclude and control confounding factors for myocardial MIBG imaging such as drugs, diabetes and structural myocardial abnormalities. Overall, the prevalence of diabetes in our study ranged from 12.5 % to 16.7% for both patients and HC. We demonstrated that in our study population the presence of the diabetes did not significantly influence differences in scintigraphy metrics. It has been postulated that a delayed H/M MIBG uptake ratio cut-off lower than 1.7 is a predictor of poor prognosis for heart disease development [31]. To reduce the possibility of including participants with significant structural heart disease or heart failure, we first performed a comprehensive review of electronic clinical records. In addition, we obtained ECG-gated ^{99m}Tc -6-MIBI SPECT images under rest conditions to identify and quantify abnormalities in global and regional myocardial perfusion, left ventricle ejection fraction, total diastolic and systolic volumes and ventricular wall movement abnormalities. All subjects with any MIBI SPECT abnormalities suggestive of structural heart disease or heart failure were subsequently evaluated by a cardiologist, who evaluated the existence of any heart conditions with a clinical interview, physical examination and appropriate ancillary evaluations (EKG and echocardiogram, among others).

There are some limitations in this study that should be mentioned. First, considering that the manuscript is based on a retrospective analysis of historical clinical data, we did not have the possibility to obtain consistent measurements on PD motor status from participants such as Unified Parkinson's Disease Rating Scale (UPDRS) or Hoehn and Yahr scores. The former clinical measures would have been extremely useful to understand the association of different motor profiles with the degrees of myocardial denervation on MIBG scintigraphies. Second, the generalizability of the proposed optimal HMR4Huptake ratio cut-offs (HMR4H_{LEHR} of 1.40 and 1.72, and HMR4H_{STD} of 1.64 and 2.15) from one imaging centre to another might be difficult, since H/M values are highly dependent on the characteristics of the collimator and on the software used and how the heart and mediastinum ROIs are placed. To overcome the variability related to the characteristics of the collimator, in addition to providing the raw HMR values calculated with our LEHR collimator, we have also included standardized HMR values adapted to the more extended and recommended ME collimators [16]. However, one should use these HMR cut-offs with caution, as other bias may be introduced in relation to variability in MIBG image acquisition and analysis methods. Third, although we reasonably discarded participants with structural heart disease or heart failure, we could not completely rule out the existence of microvascular dysfunction of the heart in all participants, an abnormality potentially inducing an impairment in myocardial sympathetic activity (MIBG uptake) and causing subtle heart failure with normal ejection fraction. Lastly, the number of patients in some of the diagnostic groups of this study (specially PARK1, PARK2 and iRBD) was small, a limitation that may have influenced the statistical power of our analyses and the generalizability of results. To overcome this limitation, we used non-parametric statistical analyses and we also worked with step-wise grouping of patients when we compared groups and when we obtained diagnostic MIBG cut-offs. It is also important to consider that genetic PD variants are rare and uncommonly identified in the clinical routine. This is especially true for SNCA-linked mutations (PARK1), which are considered a rare condition as they are limited to specific families and series around the world.

In conclusion, based on the analysis of a wide range of idiopathic and genetic variants of PD known to have differential degrees of LB pathology, our study supports the validity of myocardial MIBG scintigraphy as a *biomarker* to identify patients with LB spectrum disorders. The finding that

symptomatic carriers of PARK1 mutation have comparable delayed H/M ratios to patients with DLB and iRBD, being both diseases characterized by the presence of LBs, supports this hypothesis.

Compliance with Ethical Standards:

Funding: This study was funded by Michael J. Fox Foundation [RRIA 2014 (Rapid Response Innovation Awards) Program (Grant ID: 10189)] and Instituto de Salud Carlos III through the project "PI14/00679" and Juan Rodes grant "JR15/00008" (IG) (Co-funded by European Regional Development Fund/European Social Fund - "Investing in your future").

Conflict of Interest: Iñigo Gabilondo declares that he has no conflict of interest; Verónica Llorens declares that she has no conflict of interest; Trinidad Rodriguez declares that she has no conflict of interest; Manuel Fernández declares that he has no conflict of interest; Tomas Pérez Concha declares that he has no conflict of interest; Marian Acera declares that she has no conflict of interest; Beatriz Tijero declares that she has no conflict of interest; Ane Murueta-Goyena declares that she has no conflict of interest; Rocío del Pino declares that she has no conflict of interest; Jesús Cortés declares that he has no conflict of interest; Juan Carlos Gómez-Esteban declares that he has no conflict of interest.

Ethical approval: All procedures performed in studies involving human participants were in accordance with the ethical standards of the institutional and/or national research committee and with the 1964 Helsinki declaration and its later amendments or comparable ethical standards.

Informed consent: Informed consent was obtained from all individual participants included in the study.

References

1. Goldstein DS. Sympathetic neuroimaging. *Handb Clin Neurol*. 2013;117:365-70. doi:10.1016/B978-0-444-53491-0.00029-8.
2. Orimo S, Ozawa E, Nakade S, Sugimoto T, Mizusawa H. (123)I-metaiodobenzylguanidine myocardial scintigraphy in Parkinson's disease. *J Neurol Neurosurg Psychiatry*. 1999;67:189-94.
3. Miyamoto T, Miyamoto M, Inoue Y, Usui Y, Suzuki K, Hirata K. Reduced cardiac 123I-MIBG scintigraphy in idiopathic REM sleep behavior disorder. *Neurology*. 2006;67:2236-8. doi:10.1212/01.wnl.0000249313.25627.2e.
4. Berganzo K, Tijero B, Somme JH, Llorens V, Sanchez-Manso JC, Low D, et al. SCOPA-AUT scale in different parkinsonisms and its correlation with (123) I-MIBG cardiac scintigraphy. *Parkinsonism Relat Disord*. 2012;18:45-8. doi:10.1016/j.parkreldis.2011.08.018.
5. Taki J, Yoshita M, Yamada M, Tonami N. Significance of 123I-MIBG scintigraphy as a pathophysiological indicator in the assessment of Parkinson's disease and related disorders: it can be a specific marker for Lewy body disease. *Ann Nucl Med*. 2004;18:453-61.
6. Suzuki M, Kurita A, Hashimoto M, Fukumitsu N, Abo M, Ito Y, et al. Impaired myocardial 123I-metaiodobenzylguanidine uptake in Lewy body disease: comparison between dementia with Lewy bodies and Parkinson's disease. *J Neurol Sci*. 2006;240:15-9. doi:10.1016/j.jns.2005.08.011.
7. Kashihara K, Imamura T, Shinya T. Cardiac 123I-MIBG uptake is reduced more markedly in patients with REM sleep behavior disorder than in those with early stage Parkinson's disease. *Parkinsonism Relat Disord*. 2010;16:252-5. doi:10.1016/j.parkreldis.2009.12.010.
8. Oda H, Ishii K, Terashima A, Shimada K, Yamane Y, Kawasaki R, et al. Myocardial scintigraphy may predict the conversion to probable dementia with Lewy bodies. *Neurology*. 2013;81:1741-5. doi:10.1212/01.wnl.0000435553.67953.81.

9. Zarranz JJ, Alegre J, Gomez-Esteban JC, Lezcano E, Ros R, Ampuero I, et al. The new mutation, E46K, of alpha-synuclein causes Parkinson and Lewy body dementia. *Ann Neurol.* 2004;55:164-73. doi:10.1002/ana.10795.
10. Tijero B, Gomez-Esteban JC, Lezcano E, Fernandez-Gonzalez C, Somme J, Llorens V, et al. Cardiac sympathetic denervation in symptomatic and asymptomatic carriers of the E46K mutation in the alpha synuclein gene. *Parkinsonism Relat Disord.* 2013;19:95-100. doi:10.1016/j.parkreldis.2012.08.001.
11. Singleton A, Gwinn-Hardy K, Sharabi Y, Li ST, Holmes C, Dendi R, et al. Association between cardiac denervation and parkinsonism caused by alpha-synuclein gene triplication. *Brain : a journal of neurology.* 2004;127:768-72. doi:10.1093/brain/awh081.
12. Tijero B, Gabilondo I, Lezcano E, Teran-Villagra N, Llorens V, Ruiz-Martinez J, et al. Autonomic involvement in Parkinsonian carriers of PARK2 gene mutations. *Parkinsonism Relat Disord.* 2015;21:717-22. doi:10.1016/j.parkreldis.2015.04.012.
13. Valldeoriola F, Gaig C, Muxi A, Navales I, Paredes P, Lomena F, et al. 123I-MIBG cardiac uptake and smell identification in parkinsonian patients with LRRK2 mutations. *J Neurol.* 2011;258:1126-32. doi:10.1007/s00415-010-5896-6.
14. Nonnekes J, Timmer MH, de Vries NM, Rascol O, Helmich RC, Bloem BR. Unmasking levodopa resistance in Parkinson's disease. *Mov Disord.* 2016;31:1602-9. doi:10.1002/mds.26712.
15. Stefanelli A, Treglia G, Bruno I, Rufini V, Giordano A. Pharmacological interference with 123I-metaiodobenzylguanidine: a limitation to developing cardiac innervation imaging in clinical practice? *Eur Rev Med Pharmacol Sci.* 2013;17:1326-33.
16. Flotats A, Carrio I, Agostini D, Le Guludec D, Marcassa C, Schafers M, et al. Proposal for standardization of 123I-metaiodobenzylguanidine (MIBG) cardiac sympathetic imaging by the EANM Cardiovascular Committee and the European Council of Nuclear Cardiology. *Eur J Nucl Med Mol Imaging.* 2010;37:1802-12. doi:10.1007/s00259-010-1491-4.
17. Inoue Y, Suzuki A, Shirouzu I, Machida T, Yoshizawa Y, Akita F, et al. Effect of collimator choice on quantitative assessment of cardiac iodine 123 MIBG uptake. *J Nucl Cardiol.* 2003;10:623-32.
18. Verschure DO, Poel E, Nakajima K, Okuda K, van Eck-Smit BLF, Somsen GA, et al. A European myocardial (123)I-mIBG cross-calibration phantom study. *J Nucl Cardiol.* 2017. doi:10.1007/s12350-017-0782-6.

19. Perkins NJ, Schisterman EF. The inconsistency of "optimal" cutpoints obtained using two criteria based on the receiver operating characteristic curve. *Am J Epidemiol.* 2006;163:670-5. doi:10.1093/aje/kwj063.
20. Hall M, Frank E, Holmes G, Pfahringer A, Reutemann P, Witten A. The WEKA data mining software: an update. *J SIGKDD Explor Newsl.* 2009;11:10. doi:10.1145/1656274.1656278.
21. Schisterman EF, Perkins NJ, Liu A, Bondell H. Optimal cut-point and its corresponding Youden Index to discriminate individuals using pooled blood samples. *Epidemiology.* 2005;16:73-81.
22. Tijero B, Gomez Esteban JC, Somme J, Llorens V, Lezcano E, Martinez A, et al. Autonomic dysfunction in parkinsonian LRRK2 mutation carriers. *Parkinsonism Relat Disord.* 2013;19:906-9. doi:10.1016/j.parkreldis.2013.05.008.
23. Lamotte G, Morello R, Lebasnier A, Agostini D, Defer GL. Accuracy and cutoff values of delayed heart to mediastinum ratio with (123)I-metaiodobenzylguanidine cardiac scintigraphy for Lewy body disease diagnoses. *BMC Neurol.* 2015;15:83. doi:10.1186/s12883-015-0338-9.
24. Miyamoto T, Miyamoto M, Suzuki K, Nishibayashi M, Iwanami M, Hirata K. 123I-MIBG cardiac scintigraphy provides clues to the underlying neurodegenerative disorder in idiopathic REM sleep behavior disorder. *Sleep.* 2008;31:717-23.
25. Braune S, Reinhardt M, Schnitzer R, Riedel A, Lucking CH. Cardiac uptake of [123I]MIBG separates Parkinson's disease from multiple system atrophy. *Neurology.* 1999;53:1020-5.
26. Berg D, Postuma RB, Bloem B, Chan P, Dubois B, Gasser T, et al. Time to redefine PD? Introductory statement of the MDS Task Force on the definition of Parkinson's disease. *Mov Disord.* 2014;29:454-62. doi:10.1002/mds.25844.
27. Nagayama H, Ueda M, Yamazaki M, Nishiyama Y, Hamamoto M, Katayama Y. Abnormal cardiac [(123)I]-meta-iodobenzylguanidine uptake in multiple system atrophy. *Mov Disord.* 2010;25:1744-7. doi:10.1002/mds.23338.
28. Sone M, Yoshida M, Hashizume Y, Hishikawa N, Sobue G. alpha-Synuclein-immunoreactive structure formation is enhanced in sympathetic ganglia of patients with multiple system atrophy. *Acta Neuropathol.* 2005;110:19-26. doi:10.1007/s00401-005-1013-9.
29. Orimo S, Kanazawa T, Nakamura A, Uchihara T, Mori F, Kakita A, et al. Degeneration of cardiac sympathetic nerve can occur in multiple system atrophy. *Acta Neuropathol.* 2007;113:81-6. doi:10.1007/s00401-006-0160-y.

30. King AE, Mintz J, Royall DR. Meta-analysis of 123I-MIBG cardiac scintigraphy for the diagnosis of Lewy body-related disorders. *Mov Disord.* 2011;26:1218-24. doi:10.1002/mds.23659.
31. Nagamachi S, Fujita S, Nishii R, Futami S, Tamura S, Mizuta M, et al. Prognostic value of cardiac I-123 metaiodobenzylguanidine imaging in patients with non-insulin-dependent diabetes mellitus. *J Nucl Cardiol.* 2006;13:34-42. doi:10.1016/j.nuclcard.2005.11.009.

Figures and Figure Captions

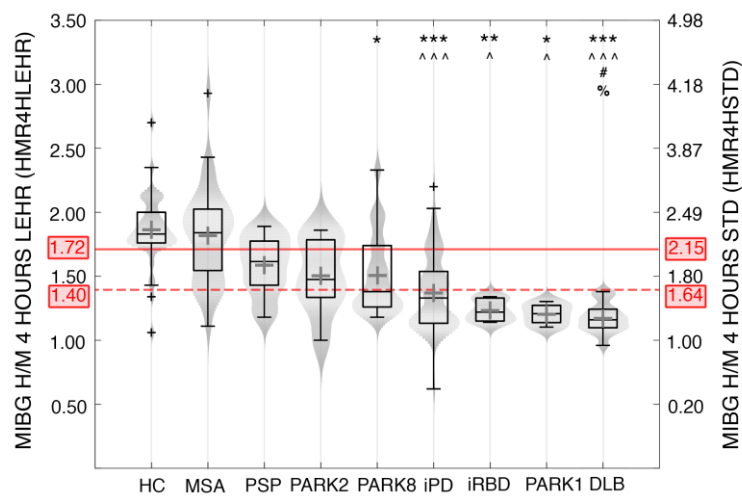


Figure 1. Boxplot and violin plot for delayed myocardial MIBG uptake ratios (HMR4H) from anterior scintigraphy images in all diagnostic groups. Within each violin, the horizontal distance between both curved boundaries and the lightness of the background at every HMR4H value represents the probability density of the HMR4H distribution in study population. MIBG: 131-I-metaiodobenzylguanidine. MIBG H/M 4 hours (HMR4H): Heart/Mediastinum ratio for myocardial MIBG uptake after 4 hours; HMR4H_{LEHR}: HMR4H values obtained with the Low Energy-High Resolution (LEHR) collimator used in the study; HMR4H_{STD}: HMR4H values calculated or standard

medium energy collimators (see methods); HC: healthy controls; MSA: multiple system atrophy; PSP: progressive supranuclear palsy; PARK2: symptomatic carriers of mutations in Parkin gene; PARK8: symptomatic carriers in LRRK2 gene; iPD: idiopathic Parkinson's disease; iRBD: idiopathic REM sleep behaviour disorder; PARK1: symptomatic carriers of E46K mutation in SNCA gene; DLB: dementia with Lewy bodies. The continuous red line indicates the optimal HMR4H_{LEHR} and HMR4H_{STD} cut-off values (1.72 and 2.15, respectively) to differentiate iPD+iRBD+PARK+DLB from HC as determined by CART and ROC analyses (see results). The discontinuous red line indicates the optimal HMR4H_{LEHR} and HMR4H_{STD} cut-off values (1.40 and 1.64, respectively) to differentiate iRBD+PARK+DLB from HC. Statistically significant ($p < 0.05$) group comparisons in Kruskal-Wallis ANOVA test are tagged as follows: 1) for comparisons with HC: * for $p < 0.05$, ** for $p < 0.005$; *** for $p < 0.001$; 2) for comparisons with MSA: ^ for $p < 0.05$, ^^ for $p < 0.005$; ^^ for $p < 0.001$; 3) for comparisons with PSP: # for $p < 0.05$; 4) for comparisons with PARK8: % for $p < 0.05$.

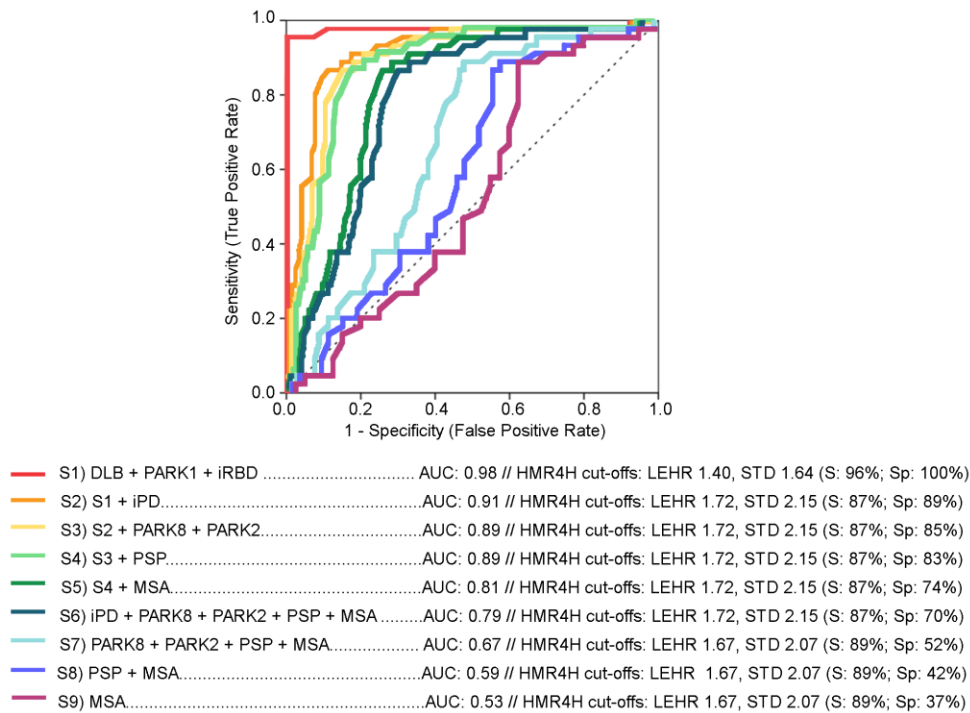


Figure 2. Non-parametric Receiver Operating Characteristic (ROC) analyses and respective optimal HMR4H cut-off values to discriminate healthy controls from patients grouped in different classification schemes. Results from non-parametric Receiver Operating Characteristic

(ROC) analyses evaluating diagnostic performance of HMR4H to discriminate healthy controls from patients clustered according to 9 classifications schemes (S1 to S9) (for further description, see the methods section). ROC curves are displayed in 9 different colours, one for each classification scheme. In addition, AUC and optimal HMR4H cut-off values with their respective sensitivity and specificity are provided for each ROC curve. AUC: area under the curve; HMR4H: late (4 hours) heart/mediastinum MIBG uptake in anterior scintigraphy images; LEHR: HMR4H values for the Low Energy-High Resolution collimator of the study; STD: HMR4H values calculated or standard medium energy collimators (see methods); S: sensitivity (%); Sp: specificity (%); MSA: multiple system atrophy; PSP: progressive supranuclear palsy; PARK2: symptomatic carriers of mutations in Parkin gene; PARK8: symptomatic carriers in LRRK2 gene; iPD: idiopathic Parkinson's disease; iRBD: idiopathic REM sleep behaviour disorder; PARK1: symptomatic carriers of E46K mutation in SNCA gene; DLB: dementia with Lewy bodies.

Table 1. Demographical data, frequency of diabetes, disease duration and myocardial MIBG uptake ratios for the early and delayed anterior scintigraphy images in all diagnostic groups

	HC	MSA	PSP	PARK2	PARK8	iPD	iRBD	PARK1	DLB
N	45	40	12	8	22	87	6	4	17
Age, years	61.84 i(11.86)	62.83 (7.96)	68.25 (6.88)	63.35 (8.64)	64.28 (10.26)	65.09 (9.95)	67.02 (4.56)	52.71 (5.93)	70.96 ^{a,h} (3.84)
Male, n (%)	22 (48.90)	18 (45.00)	7 (58.30)	3 (37.50)	12 (54.50)	50 (57.50)	5 (83.30)	2 (50.00)	10 (58.80)
Diabetes, n (%)	7 (15.90)	6 (15.00)	4 (33.30)	1 (12.50)	3 (13.60)	13 (14.90)	1 (16.70)	0	0
Disease duration, years	---	3.93 ^{d,e} (3.13)	3.55 ^d (2.07)	26.06 (13.61)	8.52 (5.36)	5.62 ^d (5.13)	3.89 (2.95)	3.94 (3.41)	4.86 (2.31)
HMR15M _{LEHR}	1.86 ^{e,f,g,h,i} (0.20)	1.83 ^{f,g,h} (0.39)	1.68 (0.16)	1.58 (0.30)	1.58 (0.31)	1.50 ^{a,b} (0.32)	1.31 ^{a,b} (0.12)	1.30 ^a (0.16)	1.36 ^{a,b} (0.18)
HMR4H _{LEHR}	1.86 ^{e,f,g,h,i} (0.26)	1.82 ^{f,g,h,i} (0.37)	1.59 ^f (0.23)	1.51 (0.30)	1.51 ^{a,h} (0.32)	1.37 ^{a,b} (0.29)	1.23 ^{a,b} (0.09)	1.20 ^{a,b} (0.09)	1.17 a,b,c,e (0.11)
HMR15M _{STD}	2.37 ^{e,f,g,h,i} (0.32)	2.34 ^{f,g,i} (0.63)	2.08 (0.25)	1.93 (0.47)	1.92 ^a (0.49)	1.79 ^{a,b} (0.51)	1.50 ^{a,b} (0.19)	1.48 ^a (0.25)	1.57 ^{a,b} (0.29)
HMR4H _{STD}	2.37 ^{e,f,g,h,i} (0.42)	2.30 ^{f,g,h,i} (0.58)	1.93 ^f (0.37)	1.81 (0.47)	1.81 ^{a,i} (0.50)	1.59 ^{a,b} (0.46)	1.37 ^{a,b} (0.14)	1.32 ^{a,b} (0.14)	1.28 a,b,c,e (0.18)
HMRW	-1.60 f,i(11.86)	-0.11 ^f (15.29)	+6.00 (10.71)	+4.30 (13.12)	+3.87 (10.85)	+8.00 a,b (10.42)	+5.51 (8.90)	+7.13 (7.25)	+11.46 ^a (0.99)

Numbers are expressed as mean (standard deviation), unless specified. HC: healthy controls; MSA: multiple system atrophy; PSP: progressive supranuclear palsy; PARK2: symptomatic carriers of mutations in Parkin gene; PARK8: symptomatic carriers in LRRK2 gene; iPD: idiopathic Parkinson's

disease; iRBD: idiopathic REM sleep behaviour disorder; PARK1: symptomatic carriers of E46K mutation in SNCA gene; DLB: dementia with Lewy bodies. HMR: heart / mediastinum ratio. HMR15M: HMR for MIBG uptake in early phase (15 min). HMR4H: HMR for MIBG uptake in delayed phase (4 hours). HMR15M_{LEHR} and HMR4H_{LEHR}: HMR15M and HMR4H calculations for the low-energy high resolution (LEHR) collimator used in the present study. HMR15M_{STD} and HMR4H_{STD}: standardized HMR15M and HMR4H values for standard medium energy collimators based on LEHR data from the present study, as determined by the formula provided by Verschure et al. (see methods section); HMRW: HMR washout of MIBG as calculated with the following formula: $[(\text{HMR15M}_{\text{LEHR}} - \text{HMR4H}_{\text{LEHR}}) / \text{HMR15M}_{\text{LEHR}}] * 100$. Statistically significant ($p < 0.05$) results in the Kruskal-Wallis ANOVA test for group comparisons: ^a versus HC; ^b versus MSA; ^c versus PSP; ^d versus PARK2; ^e versus PARK8; ^f versus iPD; ^g versus iRBD; ^h PARK1 versus; ⁱ versus DLB.

Table 2. CART classification accuracies and optimal HMR4H cut-off values to discriminate healthy controls from patients grouped in different classification schemes

	Accuracy (%) Training (Baseline)	Accuracy (%) Cross-validation	Optimal cut-off value for HMR4H _{LEHR}	Optimal cut-off value for HMR4H _{STD}
S1) DLB+ PARK1+iRBD	97.22 (62.50)	97.22	1.40	1.64
S2) S1+iPD	88.67 (71.70)	87.42	1.73	2.16
S3) S2+PARK8+PARK2	85.71 (76.19)	83.07	1,73	2.16
S4) S3+PSP	84.08 (77.61)	81.09	1.72	2.15
S5) S4+MSA	81.33 (81.33)	81.33	Not determined	Not determined
S6) iPD+PARK8+PARK2+PSP+MSA	78.97(78.97)	78.04	Not determined	Not determined
S7) PARK8+PARK2+PSP+MSA	76.38 (64.57)	62.20	Not determined	Not determined
S8) PSP+MSA	63.92 (53.61)	56.70	1.67	2.07
S9) MSA	64.71 (52.94)	57.65	1.67	2.07

Results from supervised classification of CART analyses, including accuracies and optimal cut-off values for delayed myocardial MIBG uptake ratios to differentiate healthy controls from patients clustered according to 9 classifications schemes (S1 to S9) (for further description, see methods section in the main text). Tr-Accuracy: training accuracy; Bs-Accuracy: baseline accuracy; Cv-Accuracy: cross-validation accuracy; HMR4H: delayed (4 hours) heart/mediastinum MIBG uptake ratio in anterior scintigraphy images; HMR4H_{LEHR}: HMR4H values for the original study data obtained with a Low Energy High Resolution collimator; HMR4H_{STD}: equivalent standardized HMR4H values calculated for medium energy collimators (see methods in the main text); MSA: multiple system atrophy; PSP: progressive supranuclear palsy; PARK2: symptomatic carriers of mutations in Parkin gene; PARK8: symptomatic carriers in LRRK2 gene; iPD: idiopathic Parkinson's disease; iRBD: idiopathic REM sleep behaviour disorder; PARK1: symptomatic carriers of E46K mutation in SNCA gene; DLB: dementia with Lewy bodies.